Modelling the optical properties of fresh biomass burning aerosol produced in a smoke chamber: results from the EFEU campaign

K. Hungershöfer, K. Zeromskiene, Y. Iinuma, G. Helas, J. Trentmann, T. Trautmann, R. S. Parmar, A. Wiedensohler, M. O. Andreae, O. Schmid

▶ **To cite this version:**

K. Hungershöfer, K. Zeromskiene, Y. Iinuma, G. Helas, J. Trentmann, et al.. Modelling the optical properties of fresh biomass burning aerosol produced in a smoke chamber: results from the EFEU campaign. Atmospheric Chemistry and Physics Discussions, 2007, 7 (4), pp.12657-12686. hal-00303074

HAL Id: hal-00303074
https://hal.science/hal-00303074

Submitted on 18 Jun 2008

HAL is a multi-disciplinary open access archive for the deposit and dissemination of scientific research documents, whether they are published or not. The documents may come from teaching and research institutions in France or abroad, or from public or private research centers.

L'archive ouverte pluridisciplinaire **HAL**, est destinée au dépôt et à la diffusion de documents scientifiques de niveau recherche, publiés ou non, émanant des établissements d'enseignement et de recherche français ou étrangers, des laboratoires publics ou privés.

Atmos. Chem. Phys. Discuss., 7, 12657–12686, 2007
www.atmos-chem-phys-discuss.net/7/12657/2007/
© Author(s) 2007. This work is licensed
under a Creative Commons License.

Atmospheric Chemistry and Physics Discussions

Modelling the optical properties of fresh biomass burning aerosol produced in a smoke chamber: results from the EFEU campaign

K. Hungershöfer[1,*], K. Zeromskiene[2,4], Y. Iinuma[2], G. Helas[3], J. Trentmann[5], T. Trautmann[1,6], R. S. Parmar[3], A. Wiedensohler[2], M. O. Andreae[3], and O. Schmid[3,7]

[1]Institute for Meteorology, University of Leipzig, Leipzig, Germany
[2]Leibniz-Institute for Tropospheric Research, Leipzig, Germany
[3]Max Planck Institute for Chemistry, Biogeochemistry Dept., Mainz, Germany
[4]Centre for Atmospheric Chemistry, York University, Toronto, Canada
[5]Institute for Atmospheric Physics, Johannes Gutenberg University Mainz, Mainz, Germany
[6]Remote Sensing Technology Institute, German Aerospace Centre, Wessling, Germany
[7]Institute for Inhalation Biology, GSF-National Research Centre for Environment and Health, Neuherberg, Germany
[*]now at: Laboratoire Inter-Universitaire des Systèmes Atmosphériques (LISA), Université Paris 7/12 and CNRS (UMR 7583), Créteil, France

Received: 30 July 2007 – Accepted: 22 August 2007 – Published: 29 August 2007

Correspondence to: K. Hungershöfer (hungershoefer@lisa.univ-paris12.fr)

Abstract

A better characterisation of the optical properties of biomass burning aerosol as a function of the burning conditions is required in order to quantify their effects on climate and atmospheric chemistry. Controlled laboratory combustion experiments with different fuel types were carried out at the combustion facility of the Max Planck Institute for Chemistry (Mainz, Germany) as part of the 'Impact of Vegetation Fires on the Composition and Circulation of the Atmosphere' (EFEU) project. Using the measured size distributions as well as mass scattering and absorption efficiencies, Mie calculations provided mean effective refractive indices of $1.60-0.010i$ and $1.56-0.010i$ (λ=0.55 μm) for smoke particles emitted from the combustion of savanna grass and an African hardwood (musasa), respectively. The relatively low imaginary parts suggest that the light-absorbing carbon of the investigated fresh biomass burning aerosol is only partly graphitized, resulting in strongly scattering and less absorbing particles. While the observed variability in mass scattering efficiencies was consistent with changes in particle size, the changes in the mass absorption efficiency can only be explained, if the chemical composition of the particles varies with combustion conditions.

1 Introduction

Vegetation fires in the tropics, the mid-latitudes and boreal regions are a significant source of atmospheric trace gases and aerosol particles which affect the atmospheric chemistry and the radiation budget on a global scale (Crutzen and Andreae, 1990; Andreae, 1991; Penner et al., 1992). One of the difficulties in assessing the regional and global impact of biomass burning aerosol is the fact that the physico-chemical properties of biomass burning aerosol strongly depend on the fuel characteristics, combustion conditions and the age of the smoke (Andreae and Merlet, 2001).

In the last decades, a number of biomass burning field experiments have taken

ACPD

7, 12657–12686, 2007

place in various ecosystems throughout the world, such as the South African Fire-Atmosphere Research Initiatives (SAFARI) (Lindesay et al., 1996; Swap et al., 2002), the Smoke, Clouds, and Radiation – Brazil (SCAR-B) (Kaufman et al., 1998), and the Smoke Aerosols, Clouds, Rainfall and Climate (SMOCC) campaigns in South America. Whereas the results from such field experiments always reflect a mixture of biofuels and burning conditions, laboratory experiments provide the possibility of a fuel specific characterisation of biomass emissions under controlled combustion conditions. Previous laboratory experiments dealt with the absorption properties of forest fire aerosol (Patterson and McMahon, 1984; Patterson et al., 1986), the characterisation of organic compounds (e.g., Simoneit, 2002), and emission characteristics (Christian et al., 2003). The current state of knowledge of biomass burning emissions from both field and lab experiments as well as satellite measurements, is presented in the review papers by Koppmann et al. (2005) and Reid et al. (2005a,b).

The optical properties of combustion aerosol strongly depend on particle size, shape and black carbon (BC) content and thus on fuel type and combustion conditions. Hence, the relatively wide range of optical properties for biomass burning particles reported in the literature reflects the dynamic nature of vegetation fires, variations in smoke ageing processes and – to some degree – differences in measurement techniques (Reid et al., 2005a). Consequently fundamental parameters such as the complex refractive index of the particles as well as their major constituents, namely black (or elemental) and organic carbon (OC), are highly uncertain and have to be further investigated in order to deduce the uncertainty in global estimates of direct forcing (Reid et al., 2005a).

One possibility for an improved, more thorough characterisation of particles from biomass combustion arises from performing combustion experiments in the lab. Recently, Chen et al. (2006) and Chakrabarty et al. (2006) conducted such experiments with fuels commonly burned in mid-latitude forests. Laboratory combustion experiments were also carried out as part of the 'Impact of Vegetation Fires on the Composition and Circulation of the Atmosphere' (EFEU) project (Wurzler et al., 2001;

ACPD
7, 12657–12686, 2007

Parmar et al., 2007[1]). In addition to fuels from the boreal forest region, African savanna and peat samples were investigated in the EFEU project.

The present study deals with the aerosol optical properties obtained from the combustion of African savanna grass and musasa (an African hardwood) during EFEU. The main focus of this paper is the calculation of the refractive index using Mie theory and the derivation of the apparent refractive index for the light absorbing fraction and the organic matter component. The two experiments with African fuel were selected, because tropical Africa contains about two thirds of the savanna regions worldwide and savanna fires are the largest source of biomass burning (Hao and Liu, 1994; Andreae et al., 1996).

2 Methodology

In 2003 a series of controlled combustion experiments with various types of biomass were carried out at the combustion facility of the Max Planck Institute for Chemistry in Mainz, Germany, as part of the EFEU project (Parmar et al., 2007[1]). The main goal of the experiments was the physical and chemical characterisation of the generated smoke particles. In total, 26 combustion experiments were performed during two measurement periods in summer and autumn 2003. Eight characteristic vegetation samples from different biomass burning regions were investigated including fuels from North European conifers (pine, spruce and oak), the African savanna (savanna grass and musasa) and Indonesia (peat). The reproducibility of the results was confirmed by repeating several experiments with the same fuel. In all cases the fuel moisture was very low (approximately 10%) and the size of the wood logs was relative small (thin branches, 20–40 cm long).

[1] Parmar, R. S., Frank, G., Dusek, U., et al.: A methodology for characterizing emission products from biofuel combustion: Overview of the EFEU project, J. Geophys. Res., in preparation, 2007.

ACPD
7, 12657–12686, 2007

The smoke particles were characterized with respect to a wide range of aerosol parameters including size distribution, morphology, chemical composition, mass and optical properties. The combustion conditions were monitored with concomitant CO_2 and CO measurements. Using Mie calculations and some simplifying assumptions, these data were used to derive the refractive index of both the light absorbing fraction and organic matter. Here, we concentrate on two EFEU experiments for which a maximum of information is available from the measurements, namely the combustion of savanna grass and musasa, an African hardwood. In the following, the abbreviations SAVA20a and MUSA23a, which are a combination of the fuel type and the EFEU experiment number, are used to designate the respective experiment.

2.1 Experimental Setup

The combustion facility at the Max Planck Institute for Chemistry in Mainz, Germany, is described in detail by Lobert et al. (1990) and Parmar et al. (2007)[1]. In brief, it consists of a laboratory oven with a 60 cm×60 cm burning table placed on a high-resolution balance to determine mass emission factors. The combustion emissions were drawn at a flow rate of about 3.6 m^3 min^{-1} into a 32.6 m^3 metal container which was operated as continuous flow mixing chamber with active mixing (internal fan) in order to reduce the temporal variability of the samples. The average residence time of the particles in the container was about 8 min (Parmar et al., 2007[1]). A typical burn for a given biofuel lasted about one hour and during this time new fuel material was added to the fire to maintain stable burning conditions and to guarantee a continuous flow of fresh smoke into the continuous flow mixing chamber.

2.1.1 Measurements

Gas phase measurements of carbon monoxide (CO) and carbon dioxide (CO_2) were performed directly from the mixing chamber with a non-dispersive infrared analyser (NDIR). Aerosol measurements were also performed from the mixing chamber, but

ACPD
7, 12657–12686, 2007

with a 1:20 dilution stage except for the real-time mass measurement, which was performed with a Tapered Element Oscillating Microbalance (TEOM 1400a, Thermo Scientific, NY) from a separate inlet with a 1:10 dilution stage. The TEOM was operated at a temperature of 30°C in order to minimize mass loss due to volatilization of semi-volatile aerosol compounds. The number size distribution was measured with a Scanning Mobility Particle Sizer (SMPS) and an Aerodynamic Particle Sizer (APS, TSI 3321, TSI Inc., MN) for particle diameters between 0.012–0.81 μm and 0.5–10 μm, respectively. For the two experiments considered here, the SMPS and APS data were merged without any adjustments. The total particle concentration was monitored with a condensation particle counter (CPC, TSI 3022A, TSI Inc., MN). A Berner type impactor with five size bins (0.05–0.14, 0.14–0.42, 0.42–1.2, 1.2–3.5, 3.5–10 μm) was employed to determine size-resolved particle mass and apparent elemental carbon (EC_a) mass fraction using a microbalance (Mettler Toledo, OH) and a thermographic method (C-mat 5500, Stroehlein, Germany), respectively. We use the term apparent elemental carbon (Andreae and Gelencsér, 2006) here to indicate that this species was not directly measured, but inferred from the carbon fraction that was oxidised above the temperature threshold of 650°C (Iinuma et al., 2007). An integrating nephelometer (TSI 3563, TSI Inc., MN) was employed for measurements of the scattering coefficient at three wavelengths in the visible spectral range (λ=0.45, 0.55 and 0.7 μm) and the data was corrected for the effect of angular non-idealities using Mie theory. The absorption coefficient was determined with a photo-acoustic spectrometer (PAS) at λ=0.532 μm and a particle soot absorption photometer (PSAP, Radiance Research, WA) at λ=0.565 μm. Measurements with both instruments agreed within the range of experimental uncertainty, but we will use the PAS data here, since the photo-acoustic spectrometer is less prone to measurement artefacts related to the fact that the aerosol is deposited on a filter substrate in case of the PSAP (Schmid et al., 2006). Mass scattering and absorption efficiencies in units of $m^2\,g^{-1}$ were derived by dividing the scattering coefficients obtained from the nephelometer and the absorption coefficient from the PAS measurements by the mass concentrations obtained from the TEOM. Values of the

single scattering albedo at λ=0.55 μm were calculated from the measured scattering coefficient at λ=0.55 μm and the PAS data, neglecting the small wavelength difference of the absorption coefficient. A humidified tandem differential mobility analyser (H-TDMA) was employed to determine the hygroscopic properties of the particles at initial dry diameters of 0.05, 0.1, 0.15, 0.25, 0.325 and 0.450 μm and a relative humidity of 85% (Massling et al., 2003).

To match the two minute measurement intervals of the SMPS, all temporally higher resolved measurements were averaged over the same time period. Hence the gas phase measurements, the aerosol size distribution, the total particle concentration and the optical properties are available as two-minute averages. Only the size-resolved EC_a fractions from the chemical analysis are averages over the whole duration of each continuous flow mixing experiment.

2.2 Modelling of the optical properties and derivation of refractive indices

In a first step, the measured particle size distribution and the measured scattering and absorption coefficients were used to derive an effective refractive index from Mie theory. This was accomplished by iteratively adjusting the effective complex refractive index until the calculated scattering and absorption coefficients best matched the measured ones. In a second step implications about the chemical composition were investigated based on the frequently made assumption that biomass burning particles are composed of two components, namely, non-absorbing organic carbon and strongly absorbing black carbon (Lenoble, 1991; Penner et al., 1998; Reid and Hobbs, 1998; Haywood et al., 2003). Here, the term black carbon refers to the carbon fraction which is similar to fully graphitized soot carbon with 1.75 as real part of the complex refractive index (Bond and Bergstrom, 2006). Setting the imaginary part of OC to 0 and assuming two types of mixing rules the imaginary part of the BC refractive index and the real part of the OC refractive index were obtained for various BC volume fractions between 1.5% and 15.5% by iteratively changing these parameters until the refractive index from step 1 was obtained. Hence, an estimate of the refractive indices of BC (m_{BC}) and OC

ACPD
7, 12657–12686, 2007

(m_{OC}) could be retrieved in this second step. Thereby, the effective refractive index of the OC-BC system was determined with the (internal) mixing rule of Maxwell-Garnett (MG) (Maxwell Garnett, 1904), which is preferable to simple volume mixing for particles composed of non or slightly absorbing matter containing a small amount of spherical, strongly-absorbing inclusions (Chýlek et al., 1988). Alternatively, stratified spheres with particles composed of a BC core and a shell of organic carbon assuming a constant ratio of core diameter to particle diameter were used. For both internal mixing types, the chemical composition was presumed to be the same for all sizes and constant over the whole duration of the experiment. Hence, for a given experiment temporal changes in the modelled optical properties are solely due to changes in the particle size distribution not due to variations in the chemical composition. This allows an assessment of the influence of particle size on the observed variability in the scattering and absorption coefficients.

The hygroscopic growth of the particles did not have to be considered in the model calculations, because the particles were dried to approximately 10% relative humidity by passing through the dilution system. We note that application of Mie theory requires particle sphericity, which is a reasonably good assumption for the compact particles encountered here. An estimate of a potential bias due to non-spherical particle shape will be given below. To convert the calculated optical properties into mass specific optical properties of the model particles, the experimentally determined (effective) particle density (obtained from the ratio of the TEOM mass concentration and the SMPS-APS volume concentration) was used. This ensures that the aerosol mass concentration in the model calculated from the particle number density agrees with the measured TEOM mass concentration.

3 Results

3.1 Experimental results

The measured aerosol number size distribution for both EFEU combustion experiments show a dominating and very broad accumulation mode with a maximum particle concentration for diameters between 0.1 and 0.3 μm (Fig. 1). A clear coarse mode near 3 μm is also seen. The coarse particles seem to be emitted directly from the fire, because they already appear at the very beginning of the experiment and coagulation among accumulation mode particles is slow and does not transfer particles to the coarse mode. Since coarse mode particles of crustal origin can be excluded, these large particles might be un-burnt parts of the biomass. For comparison, the diurnal average number size distribution for ambient air masses dominated by biomass burning aerosol in Amazonia obtained during the SMOCC campaign and presented in Rissler et al. (2006) is also shown in Fig. 1, where we normalized the distributions to their peak values to facilitate visual comparison. While there is good agreement between the EFEU and SMOCC data up to about 0.4 μm, higher levels of larger particles were observed for the EFEU experiments. However, the latter results from the fact that Rissler et al. (2006) only took a diameter size range from 0.022 μm up to 0.85 μm into account.

To overcome the lack of information on coarse mode particles, the scattering Ångstrom exponent was derived from the nephelometer measurements. The mean scattering Ångstrom exponents were 1.2 (SAVA20a) and 1.1 (MUSA23a) in the spectral range from λ=0.45 μm to λ=0.55 μm, or 1.8 (SAVA20a) and 2.1 (MUSA23a) from λ=0.55 μm to λ=0.70 μm (Table 1). Ångstrom exponents determined in a similar way during the Smoke, Clouds and Radiation-Brazil (SCAR-B) campaign were between 2.1 and 2.3 (0.45–0.55 μm) and between 2.4 and 2.6 (0.55–0.70 μm) (Reid and Hobbs, 1998). Hence, the smaller Ångstrom exponents for the EFEU experiments confirm the higher fraction of large particles.

The burning conditions during the course of the EFEU combustion experiments are

ACPD
7, 12657–12686, 2007

described by the CO emission ratio, $\Delta CO/\Delta CO_2$, where ΔCO and ΔCO_2 are the carbon monoxide (CO) and the carbon dioxide (CO_2) concentrations above the background level. Whereas low CO emission ratios (below approximately 11%) indicate a more complete (i.e. flaming) combustion, higher values (above approximately 11%) are typical for a less complete (smouldering) combustion. In case of SAVA20a and MUSA23a the mean $\Delta CO/\Delta CO_2$ values were 6.4% and 9.0%, respectively (Table 1), indicating that the flaming phase was dominating the particle emission. The bulk fine particle mass emission factors were 4.0 and 5.6 g kg^{-1} for the SAVA20a and MUSA23a experiment, respectively (Table 1) and thus in a range similar to previously reported values (Iinuma et al., 2007). From the chemical analysis, averaged EC_a mass fractions of 15.5% (SAVA20a) and 8.6% (MUSA23a) were retrieved, i.e. higher CO emission ratios correspond to lower EC_a fractions. This is in agreement with results from the other EFEU experiments (Iinuma et al., 2007) and with field experiments (Ferek et al., 1998). Particle diameter hygroscopic growth factors at a relative humidity (RH) of 85% were below 1.1 (MUSA23a) and smaller than 1.3 (SAVA20a) (Table 1). Because of these low growth factors we do not anticipate water to contribute significantly to the optical properties for the relative humidity encountered here (RH<10%). The single particle analysis of filter samples with a scanning electron microscope showed internally mixed particles with a compact shape (Parmar et al., 2007[1]). This justifies the model assumptions of spherical and internally mixed particles.

The mean measured mass scattering efficiencies at λ=0.55 μm were 8.9±0.2 $m^2\,g^{-1}$ and 9.3±0.3 $m^2\,g^{-1}$, for the SAVA20a and MUSA23a experiments, respectively (Table 1). The given error is the standard deviation of the mean. Mean mass scattering efficiencies varied from 6.0 $m^2\,g^{-1}$ to 12 $m^2\,g^{-1}$ for all EFEU experiments, with a mean of 9.7±2.0 $m^2\,g^{-1}$. Due to the single wavelength absorption measurements, the discussion here is restricted to a wavelength of λ=0.55 μm. The mean mass absorption efficiencies at λ=0.532 μm were 0.51±0.02 $m^2\,g^{-1}$ (SAVA20a) and 0.50±0.02 $m^2\,g^{-1}$ (MUSA23a). In general, the mean mass absorption efficiencies of the EFEU experiments ranged from 0.04 $m^2\,g^{-1}$ for peat up to 2.4 $m^2\,g^{-1}$ in case of the oak combustion,

ACPD
7, 12657–12686, 2007

but most of the mean values were below 1.0 $m^2\,g^{-1}$. For the single scattering albedo, mean values of 0.945±0.004 (SAVA20a) and 0.950±0.020 (MUSA23a) were obtained from the measurements (Table 1). In most of the EFEU cases the single scattering albedo was larger than 0.9.

3.2 Comparison with model calculations

Figures 2 and 3 show the temporal development of the $\Delta CO/\Delta CO_2$ ratio indicating the burning conditions, as well as the mass concentration and the optical properties during the combustion experiments SAVA20a and MUSA23a, respectively.

During the combustion of savanna grass, the $\Delta CO/\Delta CO_2$ values varied between 5 and 8% (Fig. 2a) with a temporal average of 6.4%, showing that the flaming phase was dominating the particle emission. The lowest CO emission ratio, and hence the most flaming combustion, was found at the beginning of the measurements at 11:29. At this time the highest mass specific absorption (Fig. 2c) and the lowest mass concentration (Fig. 2a), mass scattering (Fig. 2b) and single scattering albedo (Fig. 2d) were observed. Subsequently, the $\Delta CO/\Delta CO_2$ values increased and reached the least flaming combustion conditions at around 11:43. Likewise, the mass concentration as well as the mass scattering efficiency and the single scattering albedo increased until 11:43 as the combustion became less complete. At the same time the mass absorption efficiency decreased. After 11:43, the CO emission ratio decreased more or less continuously until the end of the combustion at 12:29 with a small local maximum around 12:23 which can be observed as a signature in the optical properties as well.

Also shown in Fig. 2 are the modelled optical properties (diamonds) for SAVA20a using a complex refractive index of $1.60-0.010i$ (λ=0.55 μm) (Table 2) that was obtained by adjusting the complex refractive index of the model particles until the averaged calculated scattering and absorption coefficients agreed with the mean of the measurements (as described in Sect. 2.2). There is generally good agreement in the temporal development of the modelled and measured optical properties, especially for

ACPD
7, 12657–12686, 2007

the mass scattering efficiency (Fig. 2b), where the calculated values are within the errors of the measurements during the whole length of the SAVA20a experiment. Similar good agreement is observed for the mass absorption efficiencies (Fig. 2c) and the single scattering albedo (Fig. 2d) except for the first 8 min and the last 5 min of the experiment where the flaming was strongest. During these two time periods the model underestimates the mass absorption, whereas the calculated mass absorption efficiency is higher than the corresponding measurements in the period around 11:45 when smouldering became more influential.

Similar results are found for the combustion of musasa (MUSA23a) presented in Fig. 3. The temporal development of the mass scattering efficiency is reproduced quite well by the model (Fig. 3b), whereas the calculated mass absorption efficiency significantly underestimates the measurements during the more flaming dominated phases at the beginning and in the middle of the experiment as can be seen in Fig. 3c. The mean effective refractive index derived for the MUSA23a experiment was $1.56-0.010i$ (Table 2).

4 Discussion

In this section the measured optical properties from the EFEU experiments SAVA20a and MUSA23a are compared with results from previous lab and field experiments. Possible reasons for differences are mentioned and evaluated. Subsequently, the measured optical properties are interpreted based on the Mie calculations and the retrieved refractive indices are discussed.

4.1 Comparison of the optical properties with results from previous measurements

Unless stated otherwise, the following brief presentation of optical properties of biomass burning particles is taken from the review paper by Reid et al. (2005a) who evaluated numerous field and laboratory measurement campaigns. According to their

ACPD
7, 12657–12686, 2007

analysis, typical in-situ measured mass scattering efficiencies in the mid-visible spectral range are between 2.8 and 4.2 $m^2 g^{-1}$ for fresh smoke in temperate, boreal and tropical forests as well as grassland fires. The mean is approximately 3.6 $m^2 g^{-1}$ and is equivalent to the value used in the IPCC Third Assessment Report (IPCC-TAR) (Houghton et al., 2001). For aged smoke, the mass scattering efficiency is about 20% higher and ranges between 3.5 and 4.6 $m^2 g^{-1}$. Literature mass absorption efficiencies for green or white light from flaming conditions are typically in the 1.0 to 1.4 $m^2 g^{-1}$ range, regardless of fuel type. For mixed phase or smouldering dominated combustion, black carbon emission is reduced, resulting in a lower mass absorption efficiency with values between 0.6–1.0 $m^2 g^{-1}$ and 0.2–0.7 $m^2 g^{-1}$, respectively. In the IPCC-TAR report mass absorption efficiencies of 0.54 and 0.45 $m^2 g^{-1}$ were assumed for fresh and aged biomass burning particles, respectively. Data on the mid-visible single scattering albedos collected from fires increase from 0.65–0.85 in the ignition/flaming phase to values of 0.8–0.9 and 0.88–0.99 for mixed phase and smouldering phase combustion, respectively.

Hence, the mass scattering efficiencies of 8.9 $m^2 g^{-1}$ and 9.3 $m^2 g^{-1}$ obtained for the SAVA20a and MUSA23a experiments are up to a factor 3 higher compared to literature values for similar burning conditions. On the other hand, the mass specific absorption efficiencies of 0.51 $m^2 g^{-1}$ (SAVA20a) and 0.50 $m^2 g^{-1}$ (MUSA23a) were lower than typical mass absorption efficiencies obtained during flaming dominated fires and agreed better with literature data for mixed phase combustions. The single scattering albedo obtained for SAVA20a (0.954) and MUSA23a (0.950) is also indicative of more strongly scattering particles compared to previously reported values from flaming dominated fires. This raises questions about the possible reasons for these deviations.

Concerning the nephelometer measurements, the reliability of the instrument was confirmed with CO_2 as calibration gas.

The actual particle shape might have an influence on the nephelometer measurements. Non-spherical particles scatter more strongly compared to ideal spheres, especially in the sideways directions, but this effect will increase the observed integrated

ACPD
7, 12657–12686, 2007

scattering signal by no more than a few percent if a particle ensemble is examined (Mugnai and Wiscombe, 1986). Hence, particle shape alone cannot explain the observed difference in mass scattering efficiency.

Another possible reason for the high mass scattering efficiencies could be an underestimation of the aerosol mass concentration. Both the TEOM and the impactors may suffer from mass loss due to the evaporation of semi-volatile particle compounds during sampling or storage. However, the following three aspects argue against a strong underestimation of the mass concentration. First, the mass concentrations observed with two different methods (impactor and TEOM) agreed within experimental uncertainties. Second, the mass emission factors of the two EFEU experiments were within the range of previously reported values. Third, an underestimation of the mass concentration should also result in an overestimation of the mass absorption efficiency. Instead, the EFEU mass absorption efficiencies were mostly smaller than the results from other flaming dominated smoke plumes.

Finally, there is the possibility that the enhanced mass scattering efficiencies are due to differences in burning conditions and/or aerosol processing. Compared to natural fires, the EFEU experiments were performed with dried biofuel and the ventilation of the fire was enhanced, since air could access the small laboratory fire from all sides. In addition, evolution of the smoke particles when flowing through the mixing chamber may lead to condensational growth due to semi-volatile organics that might enhance the mass scattering efficiencies of the particles.

In summary, serious measurement errors are unlikely to have occurred, physical particle properties like shape, dryness and size may account for some of the elevated mass scattering efficiencies, but it is likely that higher amounts of more scattering aerosol components were produced than typically reported for biomass burning aerosol due to differences in combustion conditions and/or evolution of the sample through the mixing chamber. Nevertheless, the extensive characterisation of the combustion aerosol during the controlled EFEU lab experiments offers the possibility to perform model comparisons resulting in the determination of the refractive index of

biomass burning aerosol and insights into the effect of particle size and chemistry on aerosol optical properties.

4.2 Modelling of the optical properties and retrieved refractive indices

4.2.1 Optical properties

As shown in Sect. 3.2, there is excellent agreement between the modelled and measured time series of the mass scattering efficiency for the SAVA20a combustion experiment, assuming a constant chemical composition of the model particles. For the mass absorption efficiency, the agreement is almost as good, except for the first 8 min and the last 5 min of the experiment, where the model underestimates the observed values. This is consistent with the lower $\Delta CO/\Delta CO_2$ values during this period of time probably leading to a larger black carbon fraction, which is not captured by the model, since it assumes invariant chemical composition. Figure 2d shows that the observed change in particle size does not adequately explain the measured variation in the single scattering albedo, i.e., the assumption of a constant chemical composition is only valid for almost constant burning conditions, such as observed from about 11:50 to the end of the experiment.

Good agreement between the measured and calculated optical properties was also obtained for the MUSA23a experiment, especially for the mass scattering efficiency (Fig. 3b). Similar to the SAVA20a experiment, ignoring the changing chemical composition is adequate to describe the temporal development of the mass absorption efficiency and hence the single scattering albedo during almost constant burning conditions. At times when the $\Delta CO/\Delta CO_2$ value showed the highest and lowest values, i.e. when the largest differences in the chemical composition are expected, the model is not able to reproduce the measured optical properties with the current assumptions.

ACPD
7, 12657–12686, 2007

4.2.2 Refractive indices

For the EFEU experiments SAVA20a and MUSA23a mean effective refractive indices of $1.60-0.010i$ and $1.56-0.010i$ were obtained at λ=0.55 μm (Table 2). These refractive indices have real parts which are in the upper range of values reported in the literature, where values between 1.41 and 1.59 are given. While an effective refractive index of 1.41 at λ=0.565 μm was determined for fresh smoke in the Amazon (Guyon et al., 2003), the highest real refractive indices between 1.56 and 1.59 were deduced for two biomass burning haze episodes during the Yosemite Aerosol Characterisation Study (McMeeking et al., 2005). Real parts between 1.53 and 1.58 were derived for smoke properties from laboratory combustion experiments with forest fuels (Carrico et al., 2004). Literature values for the imaginary part of the effective refractive index show a much larger variability with values between 0.0093 and 0.1 (Dubovik et al., 2002; Carrico et al., 2004; Colarco et al., 2004), and typically a smaller imaginary part was found for more smouldering combustion conditions. The values derived for the two EFEU experiments (0.010) are within the reported range, but tend to be at the lower end. This is especially worth mentioning, because the mean $\Delta CO/\Delta CO_2$ values of 6.4% (SAVA20a) and 9.0% (MUSA23a) suggest a flaming dominated combustion where larger BC fractions and imaginary parts are expected.

Beside the effective refractive index, the refractive indices of the two model components, OC (m_{OC}) and BC (m_{BC}), were derived assuming an internal mixture and BC volume fractions between 1.5% and 15.5 %. Normally, an average BC volume fraction for the model calculations is derived from the thermographic analysis, but it has to be taken into account that the apparent elemental carbon fraction obtained here (SAVA20a: 15.5%; MUSA23a: 8.6%) does not only contain black carbon, but also a non-negligible fraction of high-molecular weight light-absorbing organic material. If the measured EC_a fraction is assumed to represent an upper limit for the possible BC volume fraction, mean refractive indices of $m_{BC}=1.75-0.065i$ and $m_{OC}=1.57-0i$ have to be assumed in order to obtain the effective refractive index of $1.60-0.010i$ for the

ACPD
7, 12657–12686, 2007

EGU

SAVA20a using the Maxwell-Garnett mixing rule. In the case of MUSA23a refractive indices of m_{BC}=1.75−0.140i and m_{OC}=1.54−0i were determined (Table 2). In both cases, the imaginary parts of 0.065 and 0.140 for black carbon are very low, compared to the values between 0.1 and 1.0 given in the literature (Horvath, 1993). Assuming a stratified sphere model composed of a BC core and a concentric shell of organic material results in even lower (~20%) BC imaginary parts. This is because a stratified sphere absorbs more radiation (Bohren and Huffman, 1983), i.e. a lower imaginary part is sufficient in order to obtain the same absorption as an internal mixture using Maxwell-Garnett. If on the other hand, the black carbon is assumed to be fully graphitized having a commonly used refractive index of m_{BC}=1.75−0.630i (Bond and Bergstrom, 2006), the average BC volume fraction has to be as low as 1.5% in order to achieve an agreement between the measured and calculated optical properties (Table 2). Hence, the question arises if it could be possible that particles with a low fraction (<5%) of strongly absorbing substances were emitted, although the flaming phase was dominant during the combustion of savanna grass and musasa, and if the EC_a fraction is composed of partly graphitized and hence slightly-absorbing brown carbon instead.

The analysis of biomass burning aerosol sampled in Amazonia had already shown that a significant fraction of the aerosol mass was composed of high molecular weight organic material (Mayol-Bracero et al., 2002). It was concluded that humic-like substances (HULIS), which are used as a surrogate for brown carbon with respect to the optical properties (Andreae and Gelencsér, 2006), are generated in significant amounts during biomass burning. Hoffer et al. (2006) isolated humic-like substances from the fine biomass burning aerosol fraction collected during the SMOCC campaign in Brazil and derived a complex index of refraction at a wavelength of 0.532 μm with real parts ranging between 1.65 and 1.68 and imaginary parts from 0.00163 up to 0.00187. The emission of a significant fraction of light-absorbing brown carbon was also observed during the initial period of coal combustion (Bond, 2001). Subsequently, these pyrolysis products undergo a thermal processing leading to a progressively greater degree of graphitization. This graphitization process enhances the absorption efficiency

of the material and shifts the absorption towards longer wavelengths. A similar process might take place during the combustion of biomass - especially the lignin pyrolysis (Andreae and Gelencsér, 2006). In the case of the EFEU samples, chemical analysis using a capillary electrophoresis/electrospray ionization mass spectrometry (CE/ESI-MS) showed that the high molecular weight organic compounds that caused the high EC_a fractions were probably lignin decomposition products emitted directly from the combustion source (Iinuma et al., 2007).

Hence, we conclude that the aerosol particles from the two EFEU experiments most probably contain only a small amount of fully graphitized, strongly absorbing black carbon and instead a significant fraction of slightly-absorbing brown carbon. Indeed, the filter samples for the experiments discussed here, were rather brownish (Fig. 4).

Based on the HULIS refractive indices provided by Hoffer et al. (2006) this could explain the quite high real and the low imaginary parts of the refractive indices that were retrieved for SAVA20a and MUSA23a. Recently, Schkolnik et al. (2007) determined a low value of 0.22 for the imaginary part of the EC refractive index for biomass burning aerosol in Brazil during the SMOCC campaign, which also suggests a low graphitization level of the light-absorbing carbon.

To confirm the hypothesis that the partially graphitized carbon has a large influence on the optical properties, wavelength dependent absorption measurements would have been instructive, because the absorption of brown carbon increases towards shorter wavelengths (Hoffer et al., 2006; Andreae and Gelencsér, 2006), whereas the absorption of black carbon does not change significantly (Bergstrom and Russell, 2002). Additionally, a better characterisation of the remaining unidentified organic fraction of the combustion aerosol would contribute to clarification.

5 Summary and conclusions

As part of the 'Impact of Vegetation Fires on the Composition and Circulation of the Atmosphere' (EFEU) project, controlled combustion experiments were carried out to de-

termine the physical, chemical and optical properties of fresh biomass burning aerosol as a function of the burning conditions. The measured mass scattering efficiencies for the combustion of savanna grass (SAVA20a) and musasa (MUSA23a) at a wavelength of λ=0.55 μm were 8.9±0.2 $m^2\,g^{-1}$ and 9.3±0.3 $m^2\,g^{-1}$, respectively. For the mass absorption efficiency, values of 0.51±0.02 $m^2\,g^{-1}$ (SAVA20a) and 0.50±0.02 $m^2\,g^{-1}$ (MUSA23a) were obtained. Interestingly, the mass scattering efficiencies were up to a factor of 3 higher compared to literature data for similar flaming-dominated burning conditions, while the mass absorption efficiencies were lower than typically observed for flaming combustion, but agreed well with literature data for mixed phase combustions. This suggests that the aerosol produced under the controlled laboratory conditions consisted of more highly scattering material than typically reported for biomass burning aerosol.

Matching the observed scattering and absorption coefficients with Mie calculations based on the measured particle size distribution provided mean refractive indices for the combustion of savanna grass (SAVA20a) and musasa (MUSA23a). Assuming constant chemical composition (constant refractive index) the Mie calculations reproduced the temporal development of the measured mass scattering efficiency well. For strongly changing combustion conditions, knowledge about the temporal change of the chemical composition would be necessary to improve the agreement with the observed mass absorption efficiency and hence the single scattering albedo. The Mie calculations provided mean refractive indices of 1.60−0.010i (SAVA20a) and 1.56−0.010i (MUSA23a) (λ=0.55 μm) indicating significantly lower imaginary parts than typically found in the literature for similar burning conditions. The brown colour of the filter samples suggests that the light-absorbing carbon of the very young smoke investigated here is mostly partially graphitized carbon resulting in the measured high mass scattering and low mass absorption efficiencies. The exact reason for this is not known. We hypothesize that both differences in the combustion conditions compared to previous lab and field combustion studies and/or evolution of the sample through the mixing chamber (from which the sampling was performed) may play a role. Hence, we suggest additional

ACPD
7, 12657–12686, 2007

experiments before a possible influence of our findings on the radiation budget is investigated. For such experiments wavelength dependent absorption measurements and a better characterisation of the remaining undefined organic fraction would be instructive. Also, the combination of the thermal, optical, and solvent extraction methods is recommended in order to estimate the fraction of the strong absorbing black carbon in the determined apparent elemental carbon fraction.

Acknowledgements. This work was funded by the Federal Ministry of Education and Research (BMBF), Germany within the AFO 2000 Program under Grant 07 ATF 46 (EFEU) and by the Max Planck Society. We thank M. Welling and all the other EFEU participants for their support during the EFEU campaigns.

References

Andreae, M. O. and Gelencsér, A.: Black carbon or brown carbon? The nature of light absorbing carbonaceous aerosols, Atmos. Chem. Phys., 6, 3131–3148, 2006. 12662, 12673, 12674

Andreae, M. O. and Merlet, P.: Emission of trace gases and aerosols from biomass burning, Global Biogeochem. Cy., 14, 955–966, 2001. 12658

Andreae, M. O., Atlas, E., Cachier, H., Cofer III, W. R., Harris, G., Helas, G., Koppmann, R., Lacaux, J., and Ward, D.: Trace gas and aerosol emissions from savanna fires, in: Biomass Burning and Global Change, edited by: Levine, J., pp. 278–295, MIT Press, Cambridge, Mass., 1996. 12660

Andreae, M. O.: Biomass Burning: Its History, Use, and Distribution and Its Impact on Environmental Quality and Global Climate, in: Global Biomass Burning: Atmospheric, Climatic, and Biospheric Implications, edited by: Levine, J., pp. 3–21, MIT Press, Cambridge, Mass., 1991. 12658

Bergstrom, R. W. and Russell, P. B.: Wavelength dependence of the absorption of black carbon particles: Predictions and results from the TARFOX experiment and implications for the aerosol single scattering albedo, J. Atmos. Sci., 59, 567–77, 2002. 12674

Bohren, C. F. and Huffman, D. R.: Absorption and Scattering of Light by Small Particles, John Wiley & Sons, Inc., 1983. 12673

Bond, T. C.: Spectral dependence of visible light absorption by carbonaceous particles emitted from coal combustion, Geophys. Res. Lett., 28, 4075–4078, 2001. 12673

Bond, T. C. and Bergstrom, R. W.: Light absorption by carbonaceous particles: An investigative review, Aerosol Sci. Technol., 40, 27–67, doi:10.1080/02786820500421521, 2006. 12663, 12673

Carrico, C. M., Kreidenweis, S. M., Collett, Jr., J. L., Engling, G., and McMeeking, G. R.: Smoke Properties Derived from the Laboratory Combustion of Forest Fuels, Poster at the 23rd Annual AAAR Conference, Atlanta, Georgia, US, 2004. 12672

Chakrabarty, R. K., Moosmüller, H., Garro, M. A., Arnott, W. P., Walker, J., Susott, R. A., Babbitt, R. E., Wold, C. E., Lincoln, E. N., and Hao, W. M.: Emissions from the laboratory combustion of wildland fuels: Particle morphology and size, J. Geophys. Res., 111, D07204, doi:10.1029/2005JD006659, 2006. 12659

Chen, L.-W. A., Moosmüller, H., Arnott, W. P., Chow, J. C., and Watson, J. G.: Particle emissions from laboratory combustion of wildland fuels: In situ optical and mass measurements, Geophys. Res. Lett., 33, L04803, doi:10.1029/2005GL024838, 2006. 12659

Christian, T., Kleiss, B., Yokelson, R., Holzinger, R., Crutzen, P., Hao, W., Saharjo, B., and Ward, D.: Comprehensive laboratory measurements of biomass-burning emissions: 1. Emissions from Indonesian, African, and other fuels, J. Geophys. Res., 108, 4719, doi:10.1029/2003JD003704, 2003. 12659

Chýlek, P., Srivastava, V., Pinnick, R. G., and Wang, R.: Scattering of electromagnetic waves by composite spherical particles: Experiment and effective medium approximation, Appl. Opt., 27, 2396–2404, 1988. 12664

Colarco, P. R., Schoeberl, M. R., Doddridge, B. G., Marufu, L. T., Torres, O., and Welton, E. J.: Transport of smoke from Canadian forest fires to the surface near Washington, D.C.: Injection height, entrainment, and optical properties, J. Geophys. Res., 109, D06203, doi:10.1029/2003JD004248, 2004. 12672

Crutzen, P. J. and Andreae, M. O.: Biomass burning in the tropics: Impact on the atmospheric chemistry and biogeochemical cycles, Science, 250, 1669–1678, 1990. 12658

Dubovik, O., Holben, B., Eck, T. F., Smirnov, A., Kaufman, Y. J., King, M. D., Tanré, D., and Slutsker, I.: Variability of absorption and optical properties of key aerosol types observed in worldwide locations, J. Atmos. Sci., 59, 590–608, 2002. 12672

Ferek, R. J., Reid, J. S., Hobbs, P. V., Blake, D. R., and Liousse, C.: Emission factors of hydrocarbons, halocarbons, trace gases and particles from biomass burning in Brazil, J.

Geophys. Res., 103, 32 107–32 118, 1998. 12666
Guyon, P., Boucher, O., Graham, B., Becka, J., Mayol-Bracero, O. L., Roberts, G. C., Maenhaut, W., Artaxo, P., and Andreae, M. O.: Refractive index of aerosol particles over the Amazon tropical forest during LBA-EUSTACH 1999, J. Aerosol Sci., 34, 883–907, 2003. 12672
Hao, W. M. and Liu, M.-H.: Spatial and temporal distribution of tropical biomass burning, Global Biogeochem. Cy., 8, 495–504, 1994. 12660
Haywood, J., Osborne, S., Francis, P., Keil, A., Formenti, P., Andreae, M. O., and Kaye, P. H.: The mean physical and optical properties of regional haze dominated by biomass burning aerosol measured from the C-130 aircraft during SAFARI 2000, J. Geophys. Res., 108, 8473, doi:10.1029/2002JD002226, 2003. 12663
Hoffer, A., Gelencsér, A., Guyon, P., Kiss, G., Schmid, O., Frank, G., Artaxo, P., and Andreae, M. O.: Optical properties of humic-like substances (HULIS) in biomass-burning aerosols, Atmos. Chem. Phys., 6, 3563–3570, 2006. 12673, 12674
Horvath, H.: Atmospheric light absorption – A review, Atmos. Environ., 27A, 293–317, 1993. 12673
Houghton, J. T., Ding, Y., Griggs, D. J., Noguer, M., van der Linden, P. J., Dai, X., Maskell, K., and Johnson, C., eds.: Climate Change 2001: The Scientific Basis, Cambridge University Press, UK, 2001. 12669
Iinuma, Y., Brüggemann, E., Gnauk, T., Andreae, M. O., Helas, G., Müller, K., Parmar, R., and Herrmann, H.: Source characterization of biomass burning particles: The combustion of selected European conifers, African hardwood, savannah grass, German peat and Indonesian peat, J. Geophys. Res., 112, D08209, doi:10.1029/2006JD007120, 2007. 12662, 12666, 12674, 12681
Kaufman, Y., Hobbs, P., Kirchhoff, V., Artaxo, P., Remer, L., Holben, B., King, M., Ward, D., Prins, E., Longo, K., Mattos, L. F., Nobre, C., Spinhirne, J., Ji, Q., Thompson, A., Gleason, J., Christopher, S., and Tsay, S.-C.: Smoke, Clouds, and Radiation-Brazil (SCAR-B) experiment, J. Geophys. Res., 103, 31 783–31 808, 1998. 12659
Koppmann, R., von Czapiewski, K., and Reid, J. S.: A review of biomass burning emissions, Part I: Gaseous emissions of carbon monoxide, methane, volatile organic compounds, and nitrogen containing compounds, Atmos. Chem. Phys. Discuss., 5, 10 455–10 516, 2005. 12659
Lenoble, J.: The Particulate Matter from Biomass Burning: A Tutorial and Critical Review of Its Radiative Impact, in: Global Biomass Burning: Atmospheric, Climatic, and Biospheric

Implications, edited by: Levine, J., pp. 381–386, MIT Press, Cambridge, Mass., 1991. 12663
Lindesay, J., Andreae, M. O., Goldammer, J., Harris, G., Annegarn, H., Garstang, M., Scholes, R., and van Wilgen, B. W.: International Geosphere Biosphere Programme/International Global Atmospheric Chemistry SAFARI-92 field experiment: Background and overview, J. Geophys. Res., 101, 23 521–23 530, 1996. 12659
Lobert, J. M., Scharffe, D. H., Hao, W.-M., and Crutzen, P. J.: Importance of biomass burning in the atmospheric budgets of nitrogen-containing gases, Nature, 346, 552–554, 1990. 12661
Massling, A., Wiedensohler, A., Busch, B., Neusüss, C., Quinn, P., Bates, T., and Covert, D.: Hygroscopic properties of different aerosol types over the Atlantic and Indian Oceans, Atmos. Chem. Phys., 3, 1377–1397, 2003. 12663
Maxwell Garnett, J.: Colours in metal glasses and in metallic films, Philos. Trans. R. Soc. London, 203, 385–420, 1904. 12664, 12682
Mayol-Bracero, O. L., Guyon, P., Graham, B., Roberts, G., Andreae, M. O., Decesari, S., Facchini, M., Fuzzi, S., and Artaxo, P.: Water-soluble organic compounds in biomass burning aerosols over Amazonia. 2. Apportionment of the chemical composition and importance of the polyacidic fraction, J. Geophys. Res., D20, 8091, doi:10.1029/2001JD000522, 2002. 12673
McMeeking, G. R., Kreidenweis, S. M., Carrico, C. M., Collett, J. L., Day, D. E., and Malm, W. C.: Observations of smoke-influenced aerosol during the Yosemite Aerosol Characterization Study: 2. Aerosol scattering and absorbing properties, J. Geophys. Res., 110, D18209, doi:10.1029/2005JD005907, 2005. 12672
Mugnai, A. and Wiscombe, W. J.: Scattering from nonspherical Chebyshev particles. 1: Cross sections, single scattering albedo, asymmetry factor, and backscattered fraction, Appl. Opt., 25, 1235–1244, 1986. 12670
Patterson, E. and McMahon, C.: Absorption characteristics of forest fire particulate matter, Atmos. Environ., 18, 2541–2551, 1984. 12659
Patterson, E., McMahon, C., and Ward, D.: Absorption properties and graphitic carbon emission factors of forest fire aerosols, Geophys. Res. Lett., 13, 129–132, 1986. 12659
Penner, J., Dickinson, R., and O'Neill, C.: Effects of aerosol from biomass burning on the global radiation budget, Science, 256, 1432–1434, 1992. 12658
Penner, J., Chuang, C., and Grant, K.: Climate forcing by carbonaceous and sulfate aerosols, Clim. Dynam., 14, 839–851, 1998. 12663
Reid, J. S. and Hobbs, P. V.: Physical and optical properties of young smoke from individual

biomass fires in Brazil, J. Geophys. Res., 103, 32 013–32 030, 1998. 12663, 12665
Reid, J. S., Eck, T. F., Christopher, S. A., Koppmann, R., Dubovik, O., Eleuterio, D. P., Holben, B. N., Reid, E. A., and Zhang, J.: A review of biomass burning emissions, Part III: Intensive optical properties of biomass burning particles, Atmos. Chem. Phys., 5, 827–849, 2005a. 12659, 12668
Reid, J. S., Koppmann, R., Eck, T. F., and Eleuterio, D. P.: A review of biomass burning emissions, Part II: Intensive physical properties of biomass burning particles, Atmos. Chem. Phys., 5, 799–825, 2005b. 12659
Rissler, J., Vestin, A., Swietlicki, E., Fisch, G., Zhou, J., Artaxo, P., and Andreae, M. O.: Size distribution and hygroscopic properties of aerosol particles from dry-season biomass burning in Amazonia, Atmos. Chem. Phys., 6, 471–491, 2006. 12665, 12683
Schkolnik, G., Chand, D., Hoffer, A., Andreae, M. O., Erlick, C., Swietlicki, E. and Rudich, Y.: Constraining the density and complex refractive index of elemental and organic carbon in biomass burning aerosol using optical and chemical measurements, Atmos. Environ., 41, 1107–1118, 2007. 12674
Schmid, O., Artaxo, P., Arnott, W., Chand, D., Gatti, L., Franck, G., Hoffer, A., Schnaiter, M., and Andreae, M. O.: Spectral light absorption by ambient aerosols influenced by biomass burning in the Amazon Basin. I: Comparison and field calibration of absorption measurement techniques, Atmos. Chem. Phys., 6, 3443–3462, 2006. 12662
Simoneit, B. R. T.: Biomass burning – a review of organic tracers for smoke from incomplete combustion, Appl. Geochem., 17, 129–162, 2002. 12659
Swap, R., Annegarn, H., Suttles, J., Haywood, J., Helmlinger, M., Hely, C., Hobbs, P., Holben, B., Ji, J., King, M., Landmann, T., Maenhaut, W., Otter, L., Pak, B., Piketh, S., Platnick, S., Privette, J., Roy, D., Thompson, A., Ward, D., and Yokelson, R.: The Southern African Regional Science Initiative (SAFARI 2000): Overview of the dry season field campaign, S. Afr. J. Sci., 98, 125–130, 2002. 12659
Wurzler, S., Herrmann, H., Neusüß, C., Stratmann, F., Wiedensohler, A., Wilck, M., Trautmann, T., Andreae, M. O., Helas, G., Trentmann, J., Langmann, B., Graf, H., and Textor, C.: Impact of vegetation fires on the composition and circulation of the atmosphere: Introduction of the research project EFEU, J. Aerosol Sci., 32, Suppl. 1, S199–S200, 2001. 12659

Table 1. Temporal averages of several parameters retrieved for the EFEU combustion experiments with savanna grass (SAVA20a) and musasa (MUSA23a). In case of the optical properties the standard deviation of the mean is also given. More details on the mass emission factors can be found in Iinuma et al. (2007).

Quantity	SAVA20a	MUSA23a
$\Delta CO/\Delta CO_2$ (%)	6.4	9.0
EC_a mass fraction (%)	15.5	8.6
CPC total number concentration (10^6 cm^{-3})	3.5	4.3
Ångstrom exponent (0.45–0.55 μm)	1.2	1.1
Ångstrom exponent (0.55–0.70 μm)	1.8	2.1
TEOM mass concentration (mg m^{-3})	19.0	22.8
Scattering coefficient (m^{-1}), λ=0.55 μm	0.21±0.01	0.26±0.01
Mass scattering efficiency (m^2g^{-1}) , λ=0.55 μm	8.9±0.2	9.3±0.3
Absorption coefficient (m^{-1}), λ=0.532 μm	0.012±0.001	0.014±0.001
Mass absorption efficiency (m^2g^{-1}), λ=0.532 μm	0.51±0.02	0.50±0.02
Single scattering albedo, λ=0.55 μm	0.945 ±0.004	0.950±0.02
Mass emission factor (g kg^{-1})	4.0	5.6
Hygroscopic growth factor (RH=85%)	<1.3	<1.1

ACPD
7, 12657–12686, 2007

Table 2. Effective refractive indices (m_{eff}) and refractive indices for BC (m_{BC}) and OC (m_{OC}) which were retrieved for SAVA20a and MUSA23a using a mixture after Maxwell Garnett assuming different BC volume fractions (VF_{BC}). The wavelength is 0.55 μm.

Experiment	m_{eff}	VF_{BC}	m_{BC}	m_{OC}
	1.60−0.010*i*	0.016	1.75−0.630*i*	1.60−0*i*
SAVA20a	1.60−0.010*i*	0.10	1.75−0.105*i*	1.58−0*i*
	1.60−0.010*i*	0.155	1.75−0.065*i*	1.57−0*i*
	1.56−0.010*i*	0.015	1.75−0.630*i*	1.56−0*i*
MUSA23a	1.56−0.010*i*	0.06	1.75−0.171*i*	1.55−0*i*
	1.56−0.010*i*	0.086	1.75−0.140*i*	1.54−0*i*

ACPD
7, 12657–12686, 2007

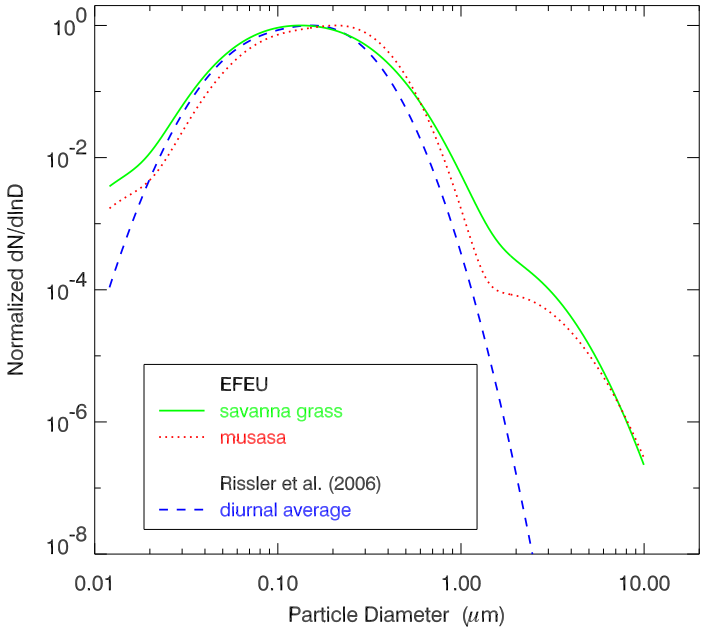

Fig. 1. Average number size distribution measured during the EFEU combustion experiments with savanna grass (SAVA20a) and musasa (MUSA23a). For comparison, the diurnal average size distribution (Aitken and accumulation mode) of ambient biomass burning aerosol measured in Brazil during the SMOCC campaign (Rissler et al., 2006) is also shown. All size distributions were normalized to their peak concentration to facilitate visual data comparison.

ACPD
7, 12657–12686, 2007

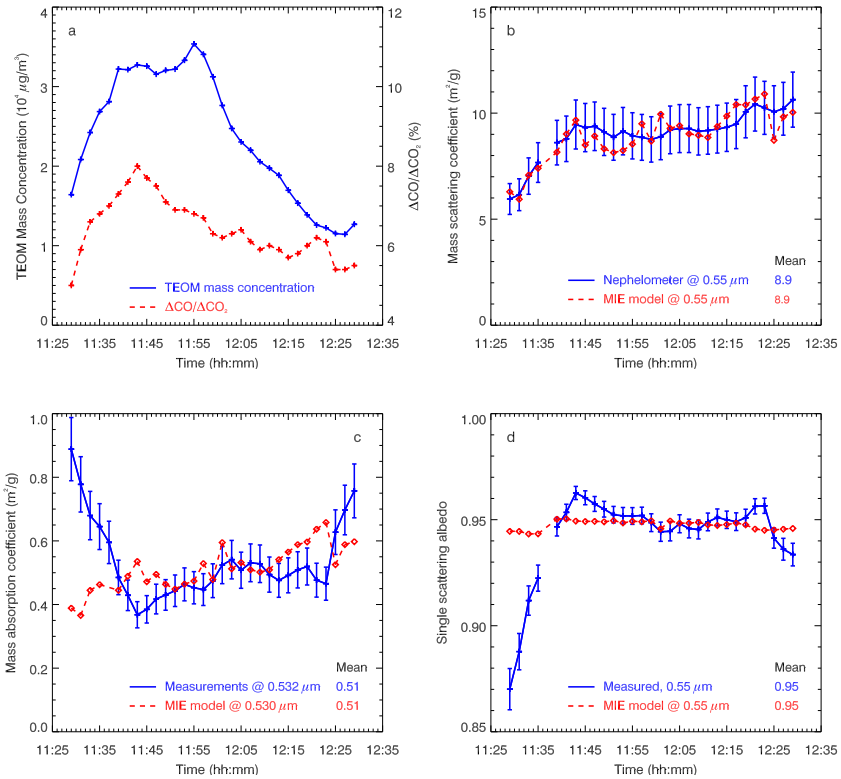

Fig. 2. Temporal development of various parameters during the combustion of savanna grass (SAVA20a): **(a)** TEOM mass concentration (left y-axis) and CO emission ratio ($\Delta CO/\Delta CO_2$) (right y-axis), **(b)** mass scattering efficiency, **(c)** mass absorption efficiency, and **(d)** single scattering albedo. For the mass concentration measured with the TEOM a 10% inaccuracy is expected. For the single scattering albedo and the mass scattering and absorption efficiency the uncertainty was calculated with the Gauss error law, assuming an uncertainty of the nephelometer and the photo-acoustic spectrometer of 7% and 5%, respectively.

ACPD
7, 12657–12686, 2007

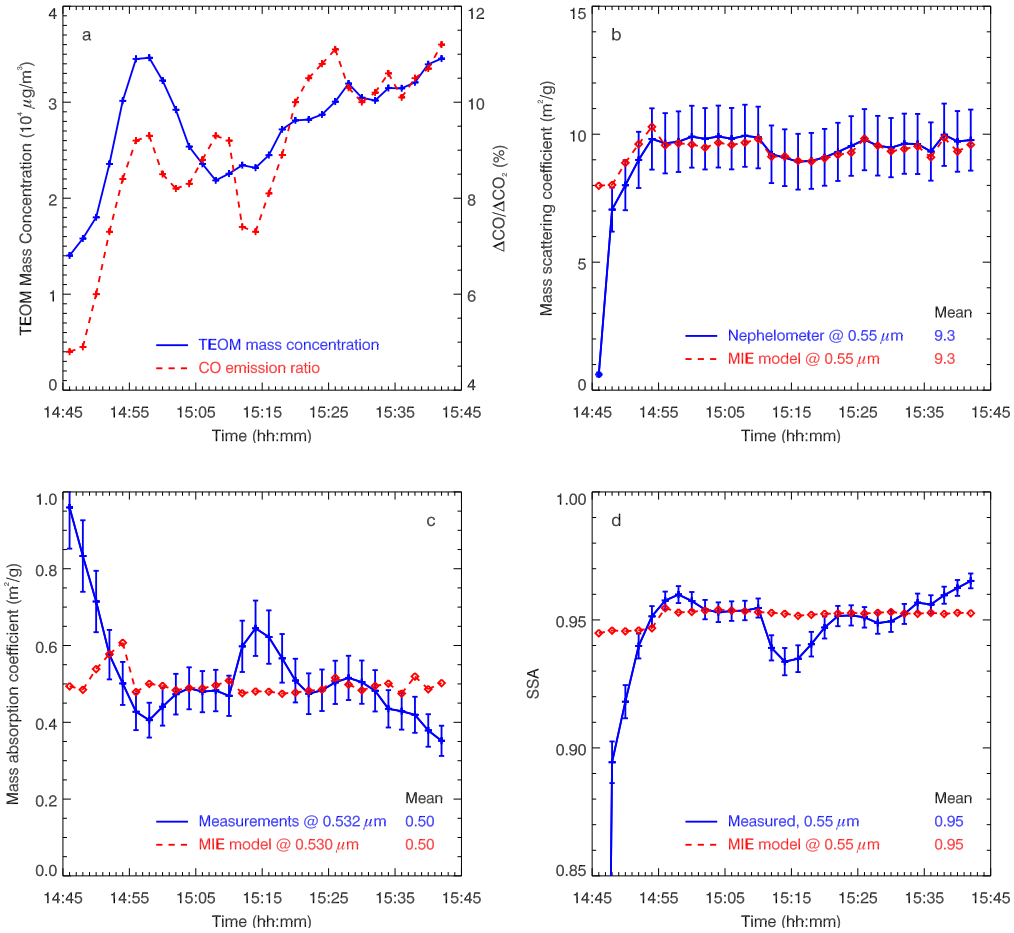

Fig. 3. Same as for Fig. 2, but for the combustion of musasa (MUSA23a).

ACPD
7, 12657–12686, 2007

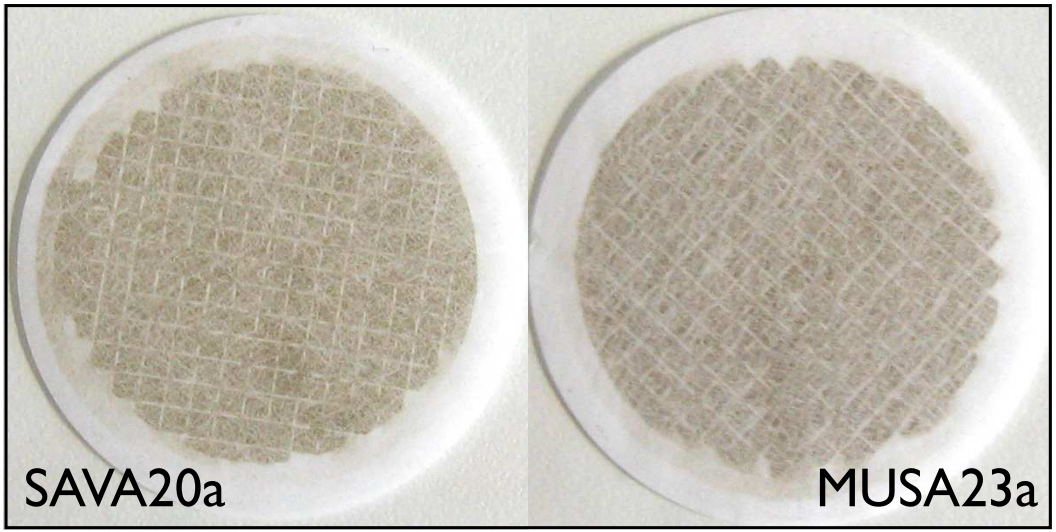

Fig. 4. Teflon filter samples from the savanna grass (left, SAVA20a) and the musasa (right, MUSA23a) combustion experiments.